

Evolution of structural and dynamic heterogeneities during elastic to plastic transition in metallic glass

L. Z. Zhao, Y. Z. Li, R. J. Xue, W. H. Wang, and H. Y. Bai^{a)}

Institute of Physics, Chinese Academy of Sciences, Beijing 100190, People's Republic of China

(Received 29 August 2015; accepted 6 October 2015; published online 21 October 2015)

We investigate the evolution of microscopically localized flow under a constant applied strain in apparent elastic region of a prototypical metallic glass (MG). The distribution and evolution of energy barriers and relaxation time spectra of the activated flow units in MG with time are obtained via activation-relaxation method. The results show that the unstable nano-scale liquid-like regions acting as flow units in the glass can be activated by external stress, and their evolution with time shows a crossover from localized activation to cascade as the proportion of the flow units reaches a critical percolation value. The flow unit evolution leads to a mechanical elastic-to-plastic transition or macroscopic plastic flow. A plausible diagram involved in time, stress, and temperature is established to understand the deformations and the flow mechanisms of MGs and could provide insights on the intriguing dilemmas of glassy nature, the flow units, and their correlations with the deformation behaviors in MGs. © 2015 AIP Publishing LLC. [<http://dx.doi.org/10.1063/1.4933343>]

I. INTRODUCTION

The structural origins of elastic and plastic deformations and relaxation behaviors of metallic glasses (MGs) have been the research focus of material science and condensed matter physics for decades.^{1–5} Intensive work concentrated on the macroscopically plastic flow in MGs.^{6–8} However, the elastic to plastic transition process under loading as well as its microstructural origin in MGs has not been paid enough attention, and its mechanism is unclear yet due to the lack of clear structural information. The plastic flow in MG is generally attributed to activated processes that involve collective motion of tens of atoms,^{9–17} which occurs initially in some local regions of shear transition zone with higher potential energy. Recent experiments and numerical simulations work of Delogu,¹⁷ Atzom,¹⁸ and Egami^{19–21} also demonstrate that when a glass subject to stress, which is much smaller than its normal yield strength, can also undergo an extremely slow flowing, which is hard to be detected within a short period of time due to the slowness.^{17–26} Besides, the glass can even flow if the time is long enough (or the strain rate is small enough), which has been confirmed by experiments in the case of lower applied stress and temperature.^{27–29} It is found that the microscopically localized flow in the apparent elastic regime of MG is markedly different from the stress-induced instantaneous flow of yielding and the subsequent plastic flow.^{22,27,28,30,31} The loading in the apparent elastic regime induces irreversible structural changes, accompanied by an increase in the stored heat of relaxation (which can be used to measure the “defects”) and marked mechanical properties change.^{27,28,30,31} The understanding of the flowing phenomena and the structural evolution path of the elastic to plastic transition with time during loading in the apparent elastic regime, especially its correlation with their mechanical

behaviors, are of crucial fundamental and practical importance. However, little work has been done on the effects of time on elastic to plastic transition in MGs due to the inaccessible long time scale.^{27,32}

Stress relaxation is a sensitive and effective instantaneous activation-relaxation technique to qualitatively investigate the properties of the flow units as well as their evolution as a function of time, temperature, and stress in MGs.^{33–37} In this work, we apply this technique to investigate the distribution and evolution of energy barriers and relaxation time of flow units in the flowing process before yielding in MG. The results clearly reveal the slow flow with the activation and evolution process of the flow units and the evolution of structural and dynamic heterogeneities. Plausible correlations among time, evolution of flow units, dynamic and structural heterogeneities, and microscopic flow to macroscopic yielding transition of MGs are established and interpreted using the perspective of flow units. A diagram involved in time, stress, and temperature is established to understand the deformations and the flow of MGs.

II. EXPERIMENTAL

We selected $Zr_{44}Ti_{11}Cu_{10}Ni_{10}Be_{25}$ (Vit1b) MG, which has large apparent elastic regime (2%), good glass-forming ability, and high thermal stability, to study the slow flow upon time. The ribbon samples were prepared by melt spinning. The structures of the as-cast alloys were ascertained by X-ray diffraction (XRD), and thermal analysis was carried out using different scanning calorimetry (DSC, Perkin-Elmer DSC8000) at a heating rate of 0.33 K/s under a constant flow of high purity argon gas. The onset temperatures of the glass transition T_g and the crystallization event T_x of $Zr_{44}Ti_{11}Cu_{10}Ni_{10}Be_{25}$ are 620 K and 747 K, respectively. To avoid the effect of the structural aging, all the samples were previously heated up to the supercooled liquid region and held for 3 min and then cooled down to

^{a)}Author to whom correspondence should be addressed. Electronic mail: hybai@iphy.ac.cn

test temperature in argon atmosphere. The stress relaxation experiments were performed on Dynamic mechanical analyzer (DMA) of TA Q800 Instruments in an argon-flushed atmosphere at 453 K. Before the experiment, 3 min delay was applied to allow the samples to equilibrate at test temperature.

III. RESULTS AND DISCUSSIONS

We apply stress relaxation method to investigate distribution and evolution of energy barriers of the activated flow units in the apparent elastic region with time. The stress decay at a constant strain of 0.4% within the nominal elastic region and the followed strain recovery after unloading at 453 K were recorded. Figure 1(a) shows representative stress relaxation experiment curve of $Zr_{44}Ti_{11}Cu_{10}Ni_{10}Be_{25}$ MG at 453 K with time of 3600 s. The stress shows a rapid decrease from the initial value and then slows down gradually with time. We unloaded the applied strain and recorded the residual strain recovery behavior subsequent to the stress relaxation processes as shown in Fig. 1(b). One can see that the total strain can be divided into two parts: elastic strain ϵ_e and inelastic strain ϵ_{ine} . The inelastic strain ϵ_{ine} can be divided into two parts: anelastic strain ϵ_a and permanent strain ϵ_p . After long time loading, permanent deformation appears and only partial applied strain recovers as exhibited in Fig. 1(b). The results indicate that the longer time stress relaxation induces permanent strain indicating irreversible atomic rearrangements and permanent deformation even in apparent elastic regime in MGs.

Figure 2(a) presents typical raw data of the stress relaxations with various time at 453 K. All the curves can be fitted by the Kohlrausch-Williams-Watts (KWW) function of $\sigma(t) = \sigma_0 \exp(-t/\tau)^\beta$, where τ is the average relaxation time and β

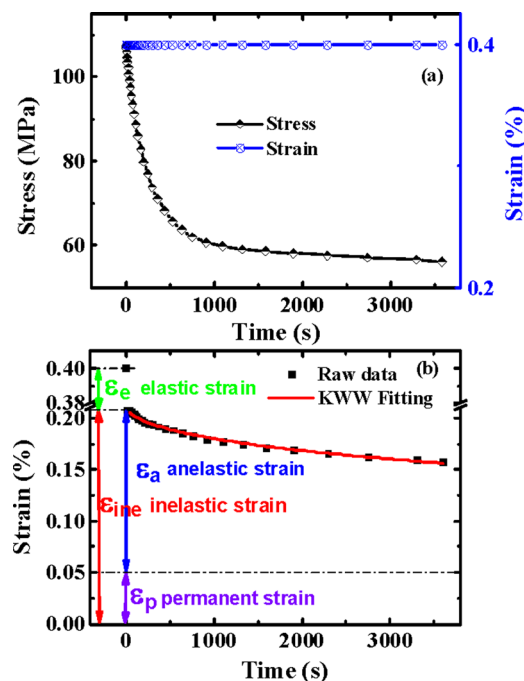


FIG. 1. (a) A typical stress relaxation curve measured at the strain of 0.4% and the test temperature is 453 K. (b) A typical recovery curve after loading for 3600 s and corresponding KWW fitting curve.

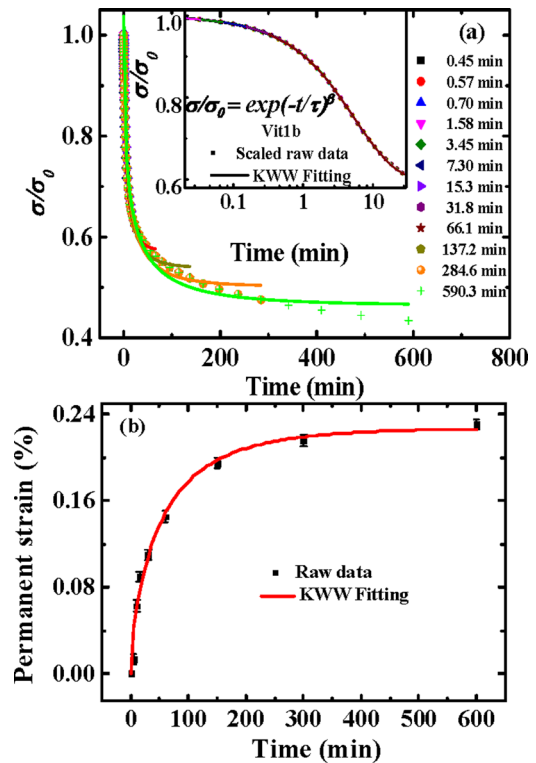


FIG. 2. (a) Typical stress relaxation curves at the strain of 0.4% for various time and the corresponding KWW fitting curves. (b) Time dependence of the permanent strain.

is a non-exponential parameter related with dynamic heterogeneity and the smaller β indicates larger dynamic heterogeneity of a system.^{38–41} The strain recovery experiments are carried out on various samples that have previously been stress relaxed at the strain of 0.4% for different times such as 300 or 36 000 s. To get the evolution of permanent strain with time, we use the KWW function of $(\epsilon_r - \epsilon_p)/(\epsilon_0 - \epsilon_p) = \exp(-t/\tau_c)^\beta$ to fit the recovery curve [see Fig. 1(b)], where τ_c is the average relaxation time, β is a non-exponential parameter, and ϵ_p is the permanent strain. From the strain recovery experiments, the evolution of the permanent strain with time is shown in Fig. 2(b), where one can find that the permanent strain increases with the increasing time in the apparent elastic regime, indicating that as the time increasing, the more applied elastic strain is converted to permanent strain in MGs.

Figure 3(a) shows the evolution of the coefficient β obtained from the KWW fitting of the stress relaxation curves upon time of the MG. Generally, the value of β decreases with increasing time, indicating the MG becomes more inhomogeneous with time. And the time dependent β evolution can be divided into two obviously different stages as indicated in Fig. 3(a), which clearly reveals the activation and evolution processes of flow units during the flow process under loading. For the short time loading, the value of β shows an exponential decay behavior (red line) and the value of β rapidly decreases to about 0.33 due to the activation and proliferation of the potential flow units in this region. As has been noted by Cheng,⁴² Demkowicz,⁴³ and Bailey *et al.*,⁴⁴ the fast exponential decay indicates a localized process, which is well consistent with the analysis above. However,

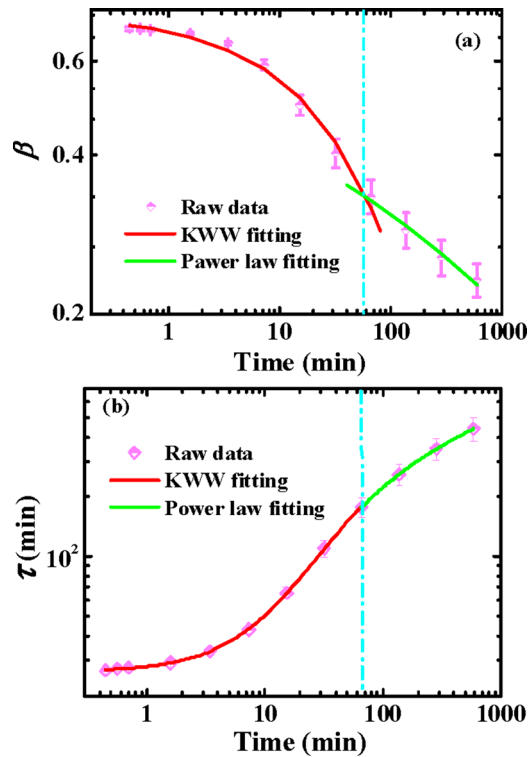


FIG. 3. (a) Time-dependent of β used for fitting stress relaxation curves. (b) Time-dependent of τ used for fitting stress relaxation curves.

with longer time (>1 h), the value of β shows a much slower power law decay behavior (green line), and the β value slowly decreases to about 0.22 due to the coalescence of the high density flow units.³³ Both experiments²² and simulations⁴⁵ in glassy materials have shown that the power law decay indicates the steady state of flow process. The results clearly exhibit the crossover from localized flow to cascades, which is related to the evolution of flow units with time in the elastic region of MG. Fig. 3(b) shows the evolution of the average relaxation time τ_c obtained from the KWW fitting of stress relaxation curves upon the time of the MG. And the time-dependent τ_c evolution also can be divided into two obviously different stages, which is similar to the change tendency of β .

The stretched exponential fashion of the stress relaxation behavior indicates that the flow units are not uniform in MGs, and the distribution and evolution of activation energy of flow units in MGs can be estimated based on the stress relaxation curves using an activation energy spectrum model.⁴⁶ The activation energy spectra of the activated flow units of the MG at various time are shown in Fig. 4(a). The apparent activation energy spectrum can be fitted by Gaussian stochastic distribution, indicating that the statistical energy barrier distribution of the flow units is heterogeneous, and only those flow units with energy barrier $E < E_c$ (the critical value of energy barrier) contribute to the flow progress. The activation energy spectra shift toward the higher value and their full width at half maximum (FWHM) increases with time, confirming more flow units with higher energy barriers are activated at longer time, which is shown in Fig. 4(b). Both the FWHM and the E_c increase during flow upon time and can also be separated as two regions,

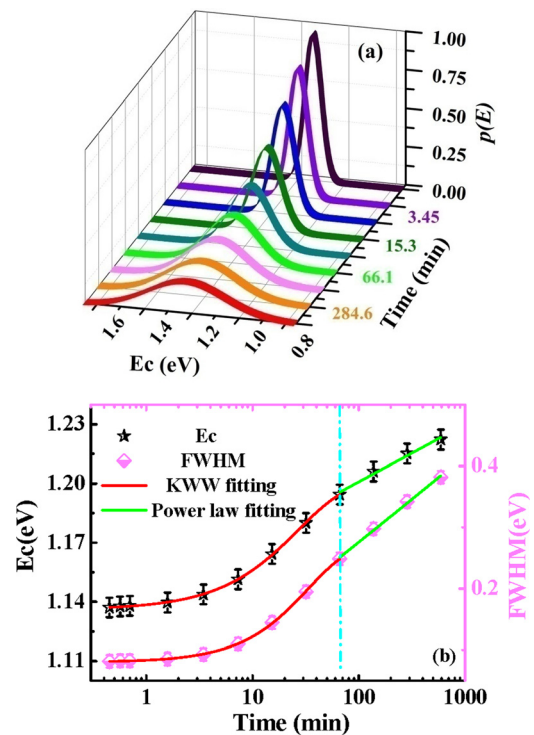


FIG. 4. (a) Time dependence of activation energy spectra $p(E)$. (b) The variation of FWHM of activation energy and activation energy spectra on time.

which is similar to the change trend of β coefficient during the flow with time, implying that the energy barrier distribution of the flow units becomes more dispersive, and more flow units with higher activation energies are engaged into the stress relaxation process at longer time. The higher fraction of liquid-like flow units makes MG more heterogeneous.

Our results demonstrate that the slow flow from elastic to plastic transition in MGs upon time can be divided into three distinct processes: the flow unit activation process at the beginning of loading (not shown here, because the activation time is very limited at this temperature and applied strain),³⁷ flow units proliferation process, and flow units coalescence process. For limited time, only few reversible flow units with smaller energy barriers and shorter intrinsic relaxation time can be activated. The isolated and reversible activation of the potential flow units accommodating the flow during elastic deformation are confined within the elastic matrix.^{23,47,48} With the increasing of time in apparent elastic regime, the flow units with higher energy barrier and larger intrinsic relaxation time are gradually activated, and the concentration of flow units increases, and this leads to the wider flow unit activation energy spectrum and more inhomogeneous,⁴⁷ corresponding to the flow units proliferation. When the time is further increased, the adjacent weak-bonded regions around flow units are also gradually transformed into liquid-like state, and the elastic shell of the isolated flow units will collapse and lead to the rapid increase of the size and fraction of the flow units. When the concentration of the flow units reaches a critical value, a connectivity percolation of flow units or liquid-like zones occurs corresponding to the coalescence process.^{23,31} At this stage, the liquid-like flow units lead to macroscopically plastic events. This process is

similar to the thermally driven glass to supercooled liquid transition³¹ and the strain induced elastic to plastic transition.⁴⁷

Our results also demonstrate that enough long time can activate more unstable and nano-scale liquid-like flow units and lead to the transition of localized flow to plastic flow in the elastic regime in glasses. According to the elastic model,^{3,49} for a flow unit with intrinsic relaxation time τ_0 , if the observation time t_0 is long ($t_0 \gg \tau_0$), the flow unit is liquid-like. However, if the observation time t_0 is very short ($t_0 \ll \tau_0$), the flow unit is solid-like. And this is the intrinsic reason for the time dependent properties of the MG. The relation of the volume fraction of flow units c and the loading time (equivalent to the observation time) t of the MG can be estimated as⁵⁰ $c = \frac{\pi^2 k T n}{8 V G \zeta \gamma_c} \ln \frac{t}{\tau_0}$, where ζ is a constant, γ_c is the yield strain limit, G is the shear modulus of the MG, T is temperature, k is the Boltzmann constant, and τ is the average relaxation time of flow units. This equation indicates that the density or the volume fraction of flow units in a MG is time dependent, and the fraction of the activated flow units become so big with extended loading time that the MG shows liquid like behavior. The result indicates that the enough long loading time can lead to homogeneous flow phenomenon even in the nominally elastic regime.⁴⁷ The loading time, which is equivalent to the stress and temperature, can result in glass transition or plastic flow in MGs.

Previous work^{12,31,50-52} and this work show that the loading time or the observation time, equivalent to temperature and stress, is one of the key parameters to glass transition or plastic deformation in MGs, and the change of any of them has equivalent role in glass transition or plastic deformation. So, a diagram of the flow for both plastic deformation and glass to liquid transformation of a MG can be constructed as shown in Fig. 5 based on the concept of flow units. We draw a horizontal cross-section through point t_0 , which represents the usual experimental observation time scale (100s) of glass transition and the temperature

corresponding to point of the usual T_g and the stress corresponding to point of the usual yield stress σ_y . The divergence in observation time axis reflects that in a sufficiently short time scale, any viscous liquid behaves like a solid glass, and a solid glass can show flow behavior or can be viewed as viscous liquid when the time scale is extended to infinite.⁴⁹ The diagram can help to rationalize and unify the description of apparently diverse transitions between liquid-like and solid-like flow behaviors in MGs.

IV. CONCLUSION

We demonstrate that, at fixed temperature and stress, enough long time can activate unstable and nano-scale liquid-like flow units and lead to the transition of localized flow to plastic flow in the apparent elastic regime in glasses. We show that the evolution process of the flow units with the loading time can be divided into three distinct processes: the flow unit activation process, proliferation process, and coalescence process. The observation time or loading time, which is equivalent to the stress and temperature, can result in glass transition or plastic deformation, and a plausible diagram involved in observation time, stress, and temperature is established to describe elastic to plastic flow or the glass transition in MGs.

ACKNOWLEDGMENTS

The financial support of the NSF of China (Grant Nos. 51271195 and 5141101072) and the MOST 973 Program (No. 2015CB856800) is appreciated. We thank P. Wen, D. Q. Zhao, M. X. Pan, and B. B. Wang for experimental assistance.

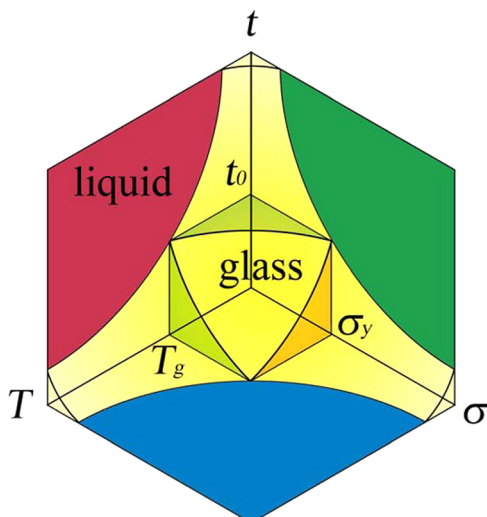


FIG. 5. Schematic of 3D glass transition or elastic to plastic transition diagram involved in observation time (corresponding to the loading time) t , temperature T , and stress σ for MGs.

¹W. Klement, R. H. Willens, and P. Duwez, *Nature* **187**, 869 (1960).

²W. Dmowski, T. Iwashita, C. P. Chuang, J. Almer, and T. Egami, *Phys. Rev. Lett.* **105**, 205502 (2010).

³P. Wen, D. Q. Zhao, M. X. Pan, and W. H. Wang, *Appl. Phys. Lett.* **84**, 2790 (2004).

⁴M. L. Falk and J. S. Langer, *Ann. Rev. Condens. Matter Phys.* **2**, 353 (2011).

⁵Y. H. Liu, G. Wang, R. J. Wang, and W. H. Wang, *Science* **315**, 1385 (2007).

⁶P. Sammonds, *Nature Mater.* **4**, 425 (2005).

⁷B. A. Sun, H. B. Yu, W. Jiao, H. Y. Bai, D. Q. Zhao, and W. H. Wang, *Phys. Rev. Lett.* **105**, 035501 (2010).

⁸B. A. Sun, S. Pauly, J. Tan, M. Stoica, W. H. Wang, U. Kuhn, and J. Eckert, *Acta Mater.* **60**, 4160 (2012).

⁹A. S. Argon and H. Y. Kuo, *J. Non-Cryst. Solids* **37**, 241 (1980).

¹⁰J. Ding, Y. Q. Cheng, and E. Ma, *Appl. Phys. Lett.* **101**, 121917 (2012).

¹¹T. Egami, T. Iwashita, and W. Dmowski, *Metals* **3**, 77 (2013).

¹²P. F. Guan, M. W. Chen, and T. Egami, *Phys. Rev. Lett.* **104**, 205701 (2010).

¹³F. Spaepen, *Acta Metall.* **25**, 407 (1977).

¹⁴W. L. Johnson and K. Samwer, *Phys. Rev. Lett.* **95**, 195501 (2005).

¹⁵J. Ye, J. Lu, C. T. Liu, Q. Wang, and Y. Yang, *Nature Mater.* **9**, 619 (2010).

¹⁶Z. Wang, P. Wen, L. S. Huo, H. Y. Bai, and W. H. Wang, *Appl. Phys. Lett.* **101**, 121906 (2012).

¹⁷F. Delogu, *Phys. Rev. Lett.* **100**, 255901 (2008).

¹⁸J. D. Ju, D. Jang, A. Nwankpa, and M. Atzmon, *J. Appl. Phys.* **109**, 053522 (2011).

¹⁹Y. Fan, T. Iwashita, and T. Egami, *Nat. Commun.* **5**, 5083 (2014).

²⁰Y. Tong, T. Iwashita, W. Dmowski, H. Bei, Y. Yokoyama, and T. Egami, *Acta Mater.* **86**, 240 (2015).

²¹Y. Fan, T. Iwashita, and T. Egami, *Phys. Rev. Lett.* **115**, 045501 (2015).

- ²²J.-O. Krisponeit, S. Pitikaris, K. E. Avila, S. Kuechemann, A. Krueger, and K. Samwer, *Nat. Commun.* **5**, 3616 (2014).
- ²³B. A. Sun, Z. Y. Liu, Y. Yang, and C. T. Liu, *Appl. Phys. Lett.* **105**, 091904 (2014).
- ²⁴S. Takeuchi and K. Edagawa, *Prog. Mater. Sci.* **56**, 785 (2011).
- ²⁵A. L. Greer, Y. Q. Cheng, and E. Ma, *Mater. Sci. Eng., R* **74**, 71 (2013).
- ²⁶J. L. Barrat and J. J. de Pablo, *MRS Bull.* **32**, 941 (2007).
- ²⁷K. W. Park, C. M. Lee, M. Wakeda, Y. Shibutani, M. L. Falk, and J. C. Lee, *Acta Mater.* **56**, 5440 (2008).
- ²⁸H. B. Ke, P. Wen, W. H. Wang, and A. L. Greer, *Scr. Mater.* **64**, 966 (2011).
- ²⁹K. Zhao, X. X. Xia, H. Y. Bai, and W. H. Wang, *Appl. Phys. Lett.* **98**, 141913 (2011).
- ³⁰T. Egami, *Prog. Mater. Sci.* **56**, 637 (2011).
- ³¹Z. Wang, B. A. Sun, H. Y. Bai, and W. H. Wang, *Nat. Commun.* **5**, 5823 (2014).
- ³²J. Lu, G. Ravichandran, and W. L. Johnson, *Acta Mater.* **51**, 3429 (2003).
- ³³T. T. Lau, A. Kushima, and S. Yip, *Phys. Rev. Lett.* **104**, 175501 (2010).
- ³⁴K. S. Lee, J. Eckert, and Y. W. Chang, *J. Non-Cryst. Solids* **353**, 2515 (2007).
- ³⁵O. P. Bobrov, S. N. Laptev, and V. A. Khonik, *Phys. Solid State* **46**, 470 (2004).
- ³⁶W. Jiao, P. Wen, H. L. Peng, H. Y. Bai, B. A. Sun, and W. H. Wang, *Appl. Phys. Lett.* **102**, 101903 (2013).
- ³⁷Z. Lu, W. H. Wang, and H. Y. Bai, *Sci. China Mater.* **58**, 98 (2015).
- ³⁸Z. Lu, W. Jiao, W. H. Wang, and H. Y. Bai, *Phys. Rev. Lett.* **113**, 045501 (2014).
- ³⁹L. Berthier, G. Biroli, J.-P. Bouchaud, L. Cipelletti, and W. van Saarloos, *Dynamical Heterogeneities in Glasses, Colloids, and Granular Media* (Oxford University Press, 2011).
- ⁴⁰M. D. Ediger, *Annu. Rev. Phys. Chem.* **51**, 99 (2000).
- ⁴¹J. S. Harmon, M. D. Demetriou, W. L. Johnson, and K. Samwer, *Phys. Rev. Lett.* **99**, 135502 (2007).
- ⁴²Y. Q. Cheng, E. Ma, and H. W. Sheng, *Phys. Rev. Lett.* **102**, 245501 (2009).
- ⁴³W. Dmowski, Y. Tong, T. Iwashita, Y. Yokoyama, and T. Egami, *Phys. Rev. B* **91**, 060101 (2015).
- ⁴⁴N. P. Bailey, T. B. Schröder, and J. C. Dyre, *Phys. Rev. Lett.* **102**, 055701 (2009).
- ⁴⁵K. M. Salerno, C. E. Maloney, and M. O. Robbins, *Phys. Rev. Lett.* **109**, 105703 (2012).
- ⁴⁶M. R. J. Gibbs, J. E. Evetts, and J. A. Leake, *J. Mater. Sci.* **18**, 278 (1983).
- ⁴⁷W. H. Wang, *J. Appl. Phys.* **110**, 053521 (2011).
- ⁴⁸L. Z. Zhao, R. J. Xue, Y. Z. Li, W. H. Wang, and H. Y. Bai, "Evolution of structural and dynamic heterogeneities during elastic to plastic transition in metallic glass" (to be published).
- ⁴⁹J. C. Dyre, *Rev. Mod. Phys.* **78**, 953 (2006).
- ⁵⁰T. P. Ge, X. Q. Gao, B. Huang, W. H. Wang, and H. Y. Bai, *Intermetallics* **67**, 47 (2015).
- ⁵¹X. Q. Gao, W. H. Wang, and H. Y. Bai, *J. Mater. Sci. Technol.* **30**, 546 (2014).
- ⁵²H. B. Yu, W. H. Wang, H. Y. Bai, and K. Samwer, *Natl. Sci. Rev.* **1**, 429 (2014).